# Magnetization of Fast and Slow Oxidized Cytochrome *c* Oxidase†

Edmund P. Day,*,‡ Jim Peterson,§ Mariana S. Sendova,‡ Jon Schoonover,∥ and Graham Palmer∥

*Department of Physics, Emory University, Atlanta, Georgia 30322, Department of Chemistry, University of Alabama, Tuscaloosa, Alabama 35487, and Department of Biochemistry and Cell Biology, Rice University, Houston, Texas 77251*

*Received December 9, 1992; Revised Manuscript Received March 30, 1993*

ABSTRACT: Oxidized cytochrome *c* oxidase can now be prepared either to react rapidly (fast) or to react slowly (slow) with cyanide [Baker, G. M., Noguchi, M., & Palmer, G. (1987) *J. Biol. Chem. 262,* 595–604]. Slow oxidized cytochrome *c* oxidase is also characterized by an integer spin $g = 12$ EPR signal which is absent in the fast form. The saturation magnetization of two samples of both forms of cytochrome oxidase has been studied at four applied magnetic fields (0.3125, 1.25, 2.5, and 5.0 T) over a temperature range from 2 to 200 K using a superconducting susceptometer. The saturation magnetization data of the two preparations are readily distinguished. The data for the coupled cytochrome $a_3$:$Cu_B$ site of both preparations are most simply interpreted as exhibiting $S = 2$ paramagnetism with $D = +13$ cm$^{-1}$ for the fast and $D = -7$ cm$^{-1}$ for the slow forms, respectively. However, there is some indication that the fast form is a mixture of both $S = 2$ and $S = 1$ paramagnetic species while the slow form is only $S = 2$.

Variability in the reactivity of oxidized bovine cytochrome oxidase (ferrocytochrome *c*:$O_2$ oxidoreductase, EC 1.9.3.1) with cyanide gave the first evidence of its heterogeneity (Van Buuren et al., 1972). Physical measurements including EPR spectroscopy (Brudvig et al., 1981) and X-ray absorption spectroscopy (Naqui et al., 1984) as well as Mössbauer spectroscopy of the oxidized bacterial (Kent et al., 1982; Rusnak et al., 1987) and the reduced yeast enzyme (Wang et al., 1988) have verified this heterogeneity. The variability in reactivity with cyanide has been used as a means of defining and preparing two separate, relatively homogeneous preparations of this enzyme. The fast form ($k' \sim 0.06$ s$^{-1}$) reacts some 300 times more rapidly with cyanide than does the slow form ($k' \sim 0.0002$ s$^{-1}$) when the oxidized cytochrome *c* oxidase is mixed with potassium cyanide (Baker et al., 1987).

Some remaining heterogeneity within the fast preparation is suggested by its reaction with NO. About 20% of the fast enzyme reacts immediately with NO to produce a $g = 6$ EPR signal, 10% is converted to ferrous cytochrome $a_3$:NO, and 70% becomes ferric low-spin cytochrome $a_3$:NO (Palmer et al., 1988). The demonstration of the existence of this additional heterogeneity in the slow form requires overnight incubation.

The increased accessibility to small molecules of the active site of the fast preparation relative to the slow is further indicated by differences in the response of the two preparations to $F^-$, $H_2O_2$, $N_3^-$, NO, and $D_2O$ (Palmer et al., 1988) as well as by their very different kinetics of reaction with $CN^-$. In each case, the observed change as indicated either by EPR (new signals in the presence of $F^-$ and NO), by shifts in the Soret band ($H_2O_2$), or by shifts in resonance Raman bands ($D_2O$) occurs much more slowly or not at all in the slow preparation.

Only a limited number of physical measurements can distinguish the fast and slow preparations of oxidized cytochrome *c* oxidase, with the $g = 12$ EPR signal being the one clear spectroscopic difference. Slow preparations have this integer EPR signal while it is absent in fast preparations. Unfortunately, this $g = 12$ signal is difficult to interpret and quantify, and is, of course, absent in the fast preparation (Hagen, 1982; Hagen et al., 1984; Brudvig et al., 1986; Hendrich et al., 1989).

In this report, we present saturation magnetization data which readily distinguish these two preparations. Our focus will be on the behavior of the coupled cytochrome $a_3$, $Cu_B$ site ($a_3$:$Cu_B$) obtained by subtracting the magnetization of the two $S = 1/2$ components, cytochrome *a* and $Cu_A$, from the primary data.

The multifield saturation magnetization study presented here is an extension of a susceptibility measurement to low temperatures (down to 2 K) and high magnetic fields (5.5 T). The new methodology (Day, 1993) results in a considerable gain in information over previous susceptibility studies which were performed at a single magnetic field often at relatively high temperatures. In those previous studies, the magnetic data had to be combined with careful metal analysis in order to determine the spin per metal site. Thus, two separate measurements were required to determine one or two magnetic properties (the spin and the exchange coupling). In the new technique, the form of the data collected over the full temperature range at several magnetic fields can be fit to determine the spin, the amount of spin, the *g* value, the zero-field splitting parameters ($D$ and $E/D$), and the exchange coupling. All of this information can be determined from the fit to the multifield saturation magnetization data alone without resorting to separate metal analysis. In the current study, the increased information of the multifield saturation magnetization method results in a clear distinction between the fast and slow forms of oxidized cytochrome *c* oxidase. A previous susceptibility study was unable to distinguish these forms of the enzyme (Barnes et al., 1991).

Previous susceptibility studies of mammalian cytochrome *c* oxidase have indicated that the high-spin $S = {}^5/_2$ ferric cytochrome $a_3$ is very strongly antiferromagnetically coupled to the spin $S = {}^1/_2$ $Cu_B$ site, yielding a net spin $S = 2$ ground state for the $a_3$:$Cu_B$ center (Tweedle et al., 1978). This observation is somewhat difficult to reconcile with the failure of synthetic chemists to prepare a model for this $a_3$:$Cu_B$ site of cytochrome *c* oxidase containing a coupled ferric–cupric

† Supported by National Institutes of Health Grants GM32394 (E.P.D.) and GM21337 (G.P.) and by the Welch Foundation (G.P.).

‡ Emory University.
§ University of Alabama.
∥ Rice University.

0006-2960/93/0432-7855$04.00/0 

pair which exhibits the large antiferromagnetic exchange coupling observed experimentally, this despite decades of effort on the their part. Furthermore, Mössbauer spectra of bacterial cytochrome *c* oxidase can be interpreted in either coupling limit—strong or weak (Rusnak et al., 1987). We will examine the saturation magnetization data in both limits in an attempt to resolve this question.

## EXPERIMENTAL PROCEDURES

*Enzymes.* Cytochrome *c* oxidase was prepared from beef heart as described previously (Baker et al., 1987); the final product gave a single rapid exponential in the cyanide assay and did not exhibit any $g = 12$ EPR signal. Enzyme concentration was determined from the absorbance of the reduced protein at 604 nm using a coefficient of 21 $mM^{-1}$ $cm^{-1}$ (per $aa_3$). Fast enzyme was converted to slow by four cycles of ammonium sulfate precipitation at pH 6.0 before being finally dissolved in the standard Hepes–DM, pH 8.0, buffer (Baker et al., 1987); the product had a Soret maximum at 417 nm and had no detectable fast phase on reaction with cyanide. A large $g = 12$ signal was apparent in the EPR spectrum recorded at 12 K. Samples were concentrated to approximately 300 $\mu$M ($aa_3$) and exchanged with deuterated buffer using Amicon filters; the concentrations of these samples were determined using a demountable cuvette with a 0.1-mm light path. The concentrations were also determined by quantifying the cytochrome *a* and $Cu_A$ EPR signals using Cu-EDTA as a primary standard.

*Magnetization Data.* Samples and controls were deuterated to eliminate noise introduced by $I = {}^1/_2$ protons, degassed to remove the paramagnetism due to molecular oxygen, and loaded into quartz holders which had been acid-etched to remove ferromagnetic impurities (Day et al., 1987). Magnetization data for both samples and controls were collected at four fields (0.3125, 1.25, 2.5, and 5 T) over the temperature range from 2 to 200 K using a Quantum Design superconducting susceptometer.

The raw data presented in Figure 1 consist of the difference of the magnetization of the sample minus its control (the filtrate from the last deuteration/concentration step). The intercepts of this difference data have been set to zero to eliminate the effects of a mismatch in the residual ferromagnetic impurities in the sample holders, a mismatch in the background diamagnetism of the sample and its control, and any temperature-independent paramagnetism.

The contributions to the magnetization arising from the independent ($S = {}^1/_2$) low- spin cytochrome *a* and $Cu_A$ sites have been subtracted from the data presented in Figures 2–5 using theoretical curves calculated with the *g* values of the well-characterized EPR signals of these sites. The amount of these background signals to be subtracted from each sample was determined initially from EPR and optical measurements; this amount was varied within the relatively large uncertainties of these measurements to examine the extent to which this background correction would impact on the fit to the $a_3$:$Cu_B$ site. Regardless of the magnitude of this correction, the fit to the resultant data was only consistent with a $S = 2$ paramagnet. Moreover, the values of the fitted parameters changed by less than the stated uncertainties. Consequently, the amount of the subtracted background used for the figures was chosen to approximate the amount of $S = 2$ paramagnetism found from the fit to the $a_3$:$Cu_B$ site through an iterative process. Theoretical magnetization curves were calculated from the appropriate spin Hamiltonian (Day et al., 1987) and fit to the data (Hendrich et al., 1991) as described previously.

Data which contains contributions from several paramagnetic species, such as the raw data of Figure 1, are presented as SI units of magnetization per sample (nJ/T sample). Data which reflect the contribution of a single spin species are presented in units of Bohr magnetons per paramagnetic center ($\beta$). In these cases (Figures 2 and 3) the amount of spin determined by fitting the data was used to establish the value of the coordinate shown on the vertical axis.

*Spectroscopy.* Electronic absorption spectra were obtained using a Cary 17 recording spectrophotometer fitted with a cell housing which would accept the narrow path length demountable cell. EPR spectra were recorded at either 77 or 12 K using a Varian E6 spectrometer.

## RESULTS AND DISCUSSION

The raw data for both fast (Figure 1A) and slow (Figure 1B) oxidized cytochrome *c* oxidase are presented in Figure 1 in plots of SI units of magnetization per sample *versus* $\beta H/kT$. The family of saturation magnetization curves is clearly distinguishable for the two samples. Similar differences were observed in data collected for a second set of samples prepared independently. These clear differences between the fast and slow preparations of oxidized cytochrome *c* oxidase which show up in the nested set of multifield saturation curves are not apparent in susceptibility data collected at a single field (Barnes et al., 1991).

The saturation magnetization data of the isolated $a_3$:$Cu_B$ site alone of fast and slow enzyme are presented in panels A and B, respectively, of Figure 2. In each case, the magnetization contributions from the cytochrome *a* and $Cu_A$ spin $S = {}^1/_2$ paramagnetism (shown as solid lines in Figure 1A,B) have been subtracted as described under Experimental Procedures.

There are two very different spin coupling models which can be used to fit the data shown in Figure 2. In the first model, the antiferromagnetic coupling between the high-spin $S = {}^5/_2$ ferric cytochrome $a_3$ site and the spin $S = {}^1/_2$ cupric $Cu_B$ site is very strong (>100 $cm^{-1}$ $\mathbf{S_1 \cdot S_2}$) to give a spin $S = 2$ system spin over the entire temperature range from 2 to 200 K. In the second model, the antiferromagnetic coupling between the two sites is very weak (<4 $cm^{-1}$ $\mathbf{S_1 \cdot S_2}$), resulting in a system which is a thermally averaged distribution over the $S = 2$ and $S = 3$ system spin states at the highest temperatures and is thus effectively uncoupled, at least with respect to this susceptibility measurement.

From the form of the data alone (Figure 2), one cannot rule out either the strong or the weak coupling alternatives; both models can fit the data. However, the quantity of binuclear metal center required to fit the data is very different in the two cases. The strong coupling model results in a fit in which the amount of dimer matches the amount of protein in the sample within the uncertainties. By contrast, the weak coupling model results in a fit in which the predicted amount of dimer is substantially less than the amount of protein in the sample (<65%, see last column of Table II). This difference can be understood by considering the high-temperature slope which is proportional to $g^2S(S + 1)$. The value of $g^2S(S + 1)$ is 24 for the strong coupling model where the $a_3$:$Cu_B$ site is exclusively spin $S = 2$. However, with the weak coupling model, the system spin is thermally randomized over the coupled $S = 2$ and $S = 3$ states, and at high temperatures, the net value of $g^2S(S + 1)$ is $(5/12)24 + (7/12)48$. This is the same value ($g^2S(S + 1) = 38$) as would be obtained from a magnetically isolated $S = {}^5/_2$ plus $S = {}^1/_2$ pair. Clearly, substantially less ($24/38 \sim 63\%$) of the weakly coupled $a_3$:$Cu_B$ site is required to fit the data. Thus, for this weak coupling model to match the data, a substantial fraction (>35%) of the iron would have to be present as a low-spin $S = {}^1/_2$ ferric

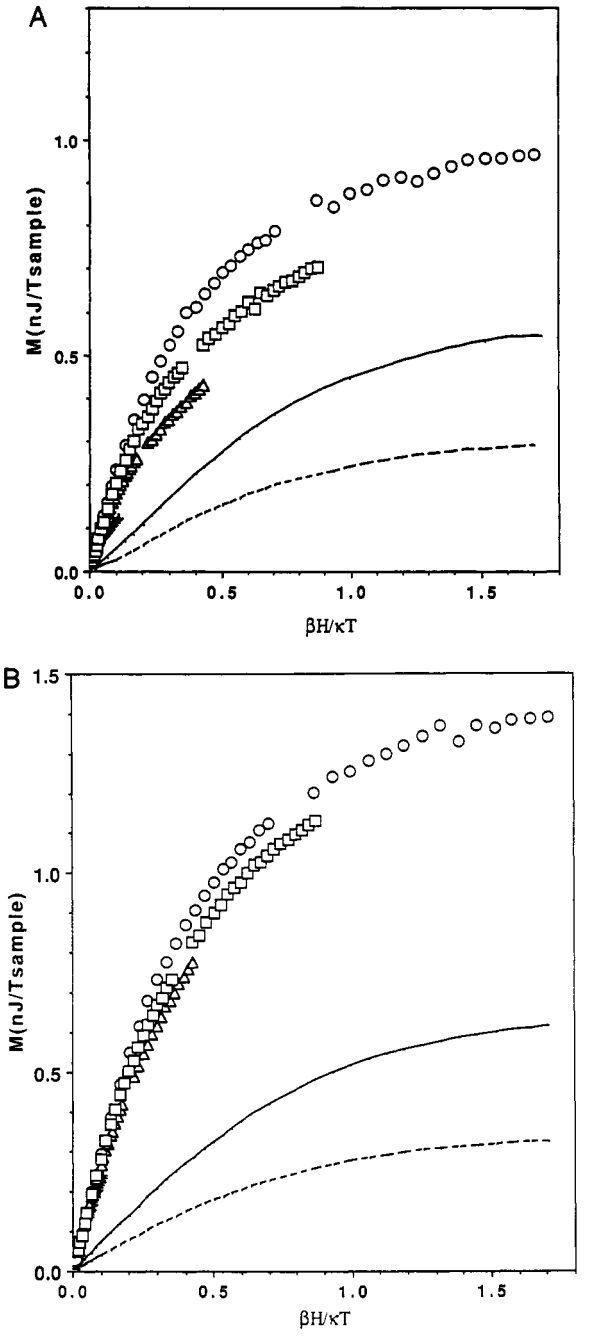


FIGURE 1: Saturation magnetization of oxidized cytochrome *c* oxidase (sample 2) at four fields [(○) 5.0, (□) 2.5, (△) 1.25, and (+) 0.313 T] over the temperature range from 2 to 200 K plotted in SI units per sample ($nJ/T$ sample) against $\beta H/kT$. Raw data for (A) fast and (B) slow samples are shown separately with the maximum value of the vertical axes chosen to account for the slightly different amounts of protein in the two samples. The amount of magnetization contributed by the cytochrome *a* (dashed lines) and $Cu_A$ sites is indicated by a solid line in each figure.

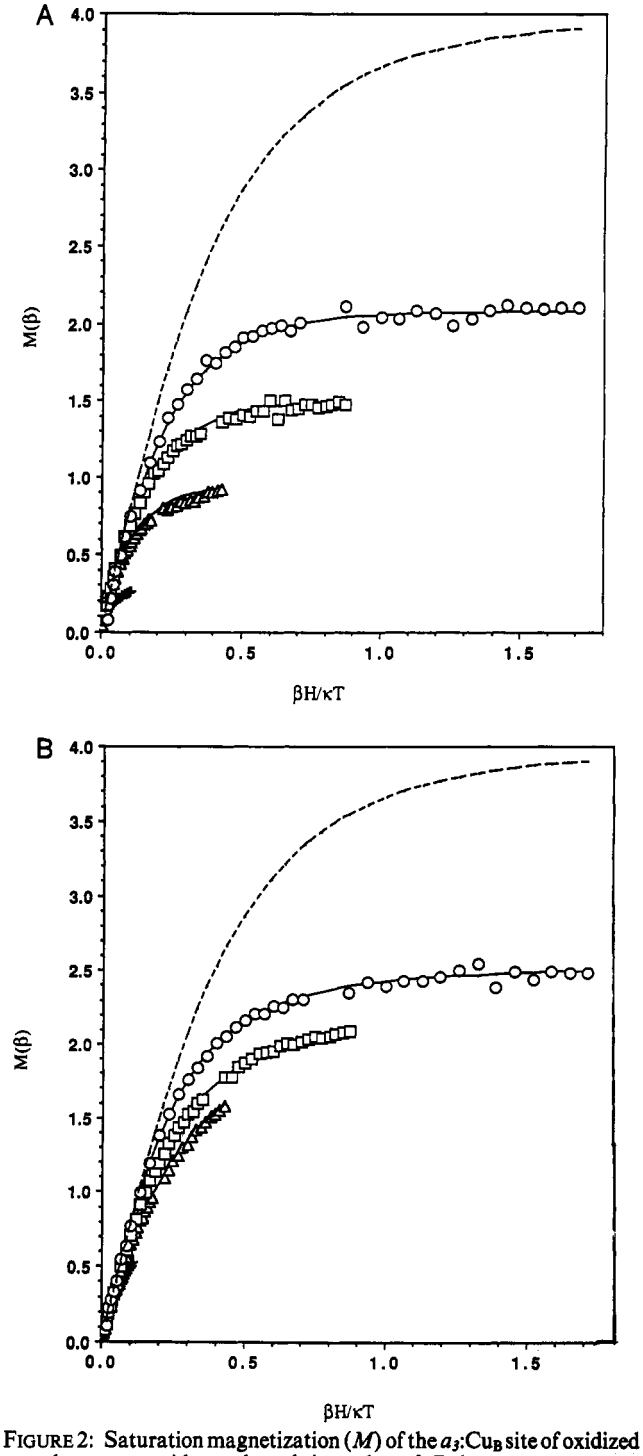


FIGURE 2: Saturation magnetization ($M$) of the $a_3$:$Cu_B$ site of oxidized cytochrome *c* oxidase plotted in units of Bohr magnetons per paramagnetic center ($\beta$) against $\beta H/kT$. The symbols have the same meaning as in Figure 1. The magnetization contributions of the cytochrome *a* and $Cu_A$ sites of (A) fast and (B) slow preparations have been subtracted from the data shown in Figure 1. The solid lines were found by fitting the data with theoretical magnetization curves calculated without approximation from a spin $S = 2$ Hamiltonian. The dashed lines are the Brillouin curves calculated with $D = E = 0$. The vertical axes were scaled using the amount of spin $S = 2$ determined from the fit. The zero-field splitting parameters for the fits were as follows: (A) fast, $S = 2$, $D = 13$ cm$^{-1}$, $E/D = 0.23$, $g = 2.0$; (B) slow, $S = 2$, $D = -7.4$ cm$^{-1}$, $E/D = 0.27$, $g = 2.0$.

cytochrome $a_3$ strongly coupled antiferromagnetically to the spin $S = {}^1/_2$ cupric site to give a diamagnetic $S = 0$ system spin. Surprisingly then, the weak coupling model does not escape the strong coupling dilemma since it too requires a contribution from strong coupling between the ferric and cupric sites to produce this diamagnetic component. We will present the strong coupling model first.

*Strong Antiferromagnetic Exchange Coupling.* The solid lines of Figure 2 were determined by fitting the data with a spin $S = 2$ Hamiltonian. Although other spins were tried, the spin $S = 2$ system was the only spin that fit the data under the assumption that the $a_3$:$Cu_B$ site consisted of a single paramagnetic center. Moreover, the amounts of spin $S = 2$ species found from the fits to the saturation magnetization data were within the uncertainties of the amounts of protein determined from both EPR and optical measurements on each sample. The successful fit using spin $S = 2$ indicates that the high-spin $S = {}^5/_2$ ferric $a_3$ heme is coupled strongly with the $S = {}^1/_2$ $Cu_B$ site to produce the observed net spin $S = 2$ site

in both the fast and the slow samples. The fact the spin $S$ = 2 Hamiltonian fits the data over the entire temperature range (2–200 K) indicates that the exchange coupling is large (>100 $cm^{-1}$ $S_1 \cdot S_2$). Earlier single-field susceptibility studies of oxidized cytochrome *c* oxidase are consistent with this saturation magnetization result (Tweedle et al., 1978; Moss et al., 1978; Barnes et al., 1991).

The saturation behavior of the $a_3$:$Cu_B$ site of fast and slow samples is dramatically different as can be seen by inspection of Figures 1, 2, or 3 and as evidenced by the very different zero-field splittings determined from the fits to the data shown in Figure 2. The best fit to the $a_3$:$Cu_B$ site of sample 2 of fast oxidized cytochrome *c* oxidase yields a zero-field splitting parameter ($D$)[1] of 13 $cm^{-1}$ with a ratio of the rhombic to axial zero-field parameters ($E/D$)[2] of 0.23. By contrast, the best fit to the $a_3$:$Cu_B$ site of sample 2 of slow oxidized cytochrome *c* oxidase yields a $D$ of –7.4 $cm^{-1}$ with an $E/D$ of 0.27. The change in sign of the zero-field splitting parameter upon conversion from fast enzyme to slow enzyme is most surprising. It should be noted, however, that at the limit of $E/D$ = 1/3 the sign of $D$ is undefined. As the value of $E/D$ determined by the fitting process is close to this rhombic limit, it may be that the difference in sign is only apparent.

Fits to saturation magnetization data are incapable, on their own, of defining sample homogeneity. While both the raw data of Figure 1 and the $a_3$:$Cu_B$ data of Figure 2 make it clear that saturation magnetization can readily distinguish fast from slow oxidized cytochrome *c* oxidase, it is not possible to conclude from the magnetization data alone whether or not the measured $D$ and $E/D$ values represent the intrinsic molecular properties of each of the two samples or reflect different averages of heterogeneous molecular populations.

The $g$ = 12 EPR signal of the slow preparation is difficult to reconcile with the $D$ (–7.4 $cm^{-1}$) and $E/D$ (0.27) values found from the fit to the data of Figure 2. On the presumption that the $g$ = 12 signal in cytochrome oxidase has the same origin as that seen in other heme proteins (Hendrich et al., 1989), the presence of this resonance requires that the magnitude of the quantity $4E^2/D$ must be less than or equal to the X-band microwave quantum (0.3 $cm^{-1}$). In this case, the magnitude of the quantity $4E^2/D$ (2.2 $cm^{-1}$) is far greater than the X-band quantum. This suggests that the $g$ = 12 signal arises from a subpopulation of the slow sample which has a much smaller $E/D$ (<0.1) than that determined for the sample as a whole. Taken together, the best fit to the saturation magnetization data combined with the integer EPR data of slow oxidized cytochrome *c* oxidase indicates heterogeneity in the observed $S$ = 2 species.

The saturation magnetization data and the fits at the lowest field for both the fast (A) and the slow (B) oxidized cytochrome *c* oxidase are shown in Figure 3. This figure highlights both the differences between the data for the fast and the slow samples and the fact the fit to the fast sample for spin $S$ = 2 is not of the same quality as that of the slow sample. Only the lowest field data are shown in Figures 3– 5 to highlight these differences. However, in each case, the solid line was found by fitting the entire family of curves at all four fields.

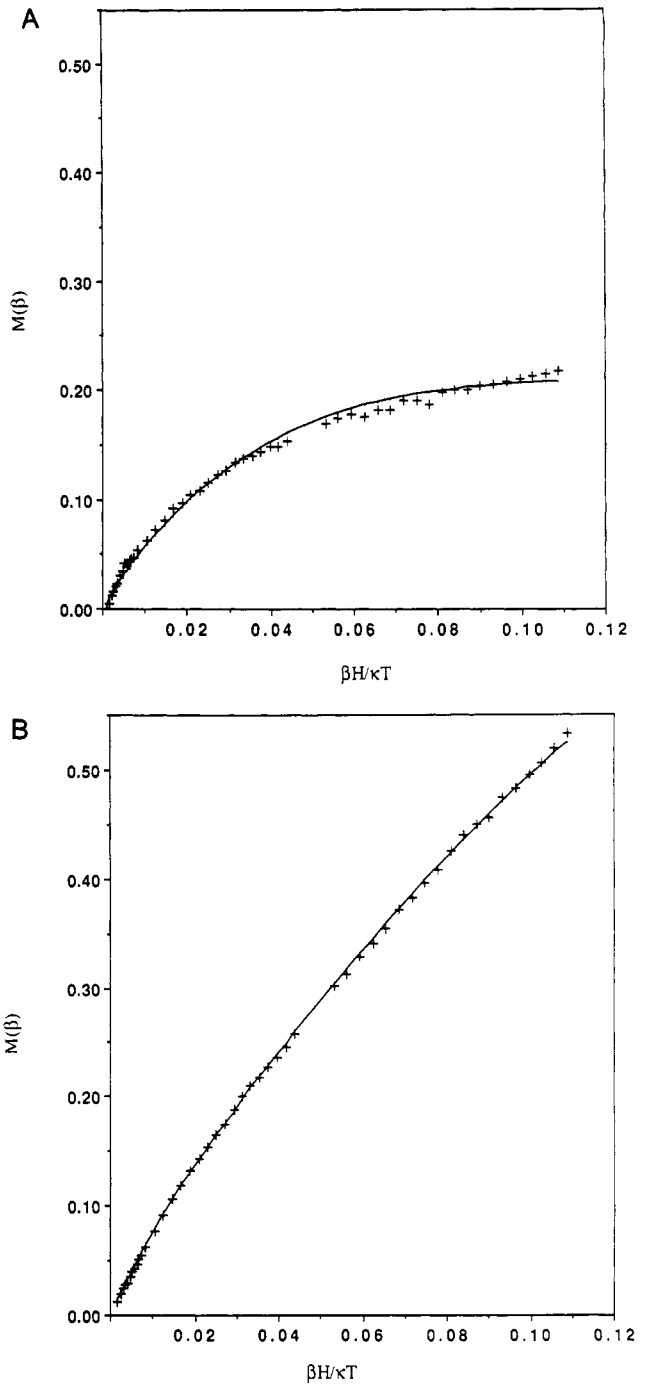


FIGURE 3: Lowest field (+0.313 T) saturation magnetization of the $a_3$:$Cu_B$ site of (A) fast and (B) slow oxidized cytochrome *c* oxidase. These data have been selected from Figure 2 for separate presentation to emphasize the differences between the two preparations and to indicate the shortcoming in the spin $S$ = 2 fit to the fast data.

At the risk of overinterpreting the data, we have extended the analysis of the fast sample to include a second spin. The results of this analysis are shown in Figure 5. Because the data are being treated as arising from a composite of two spins, the magnetization data are presented in SI units per sample ($nJ/T$ sample) rather than as Bohr magnetons per paramagnetic center ($\beta$). The data of Figure 3A have been presented in Figure 4 against this same vertical scale for direct comparison with Figure 5. In the case of the fast sample but not in the case of the slow sample, the spin $S$ = 2 only fit is improved by assuming that a majority (75%) of the sample is in the $S$ = 1 spin state with the remainder of the fast sample

[1] The zero-field splitting parameter ($D$) referred to throughout this paper was measured by fitting the data for the $a_3$:$Cu_B$ site and is that of the coupled site. The value of the zero-field splitting parameter for the high-spin Fe(III) site ($D_1$) is found from the expression $D = (4/3)D_1$ (Scaringe et al., 1978).

[2] The values of $E/D$ found from the best fits to the data for sample 2 are given in the text and in the figure legends. This parameter is soft. No values for $E/D$ are given in Table I, and the stated uncertainties for the other parameters in the table are consistent with allowing $E/D$ to vary over its entire range from 0 to 1/3. These uncertainties in the other parameters are similar to those found by averaging results for the best fits to two independent preparations of either fast or slow enzyme.

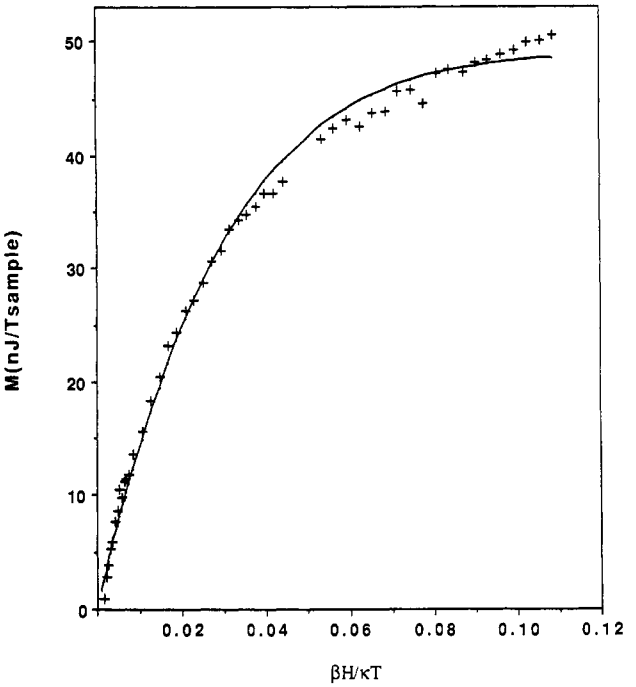


FIGURE 4: Lowest field (+0.313 T) data and spin $S = 2$ fit for fast oxidized cytochrome *c* oxidase of Figure 3A have been replotted in SI units of magnetization per sample against $\beta H/kT$ for comparison with Figure 5.

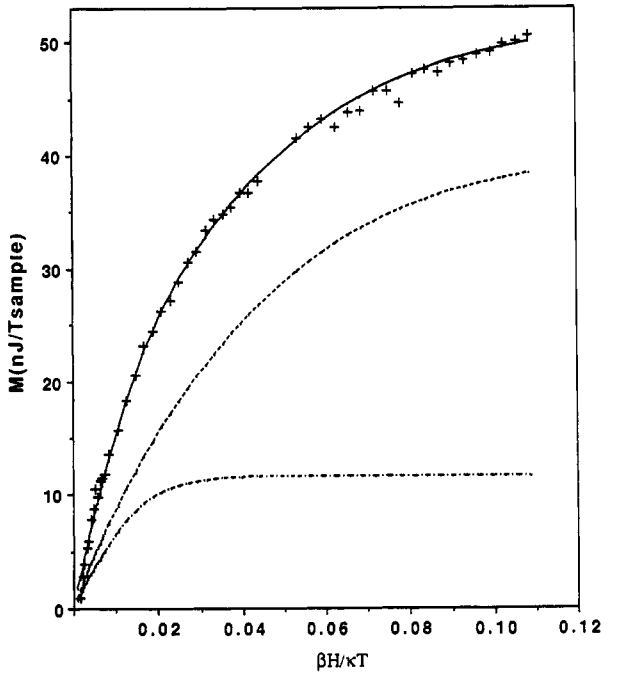


FIGURE 5: Lowest field (+0.313 T) data for fast oxidized cytochrome *c* oxidase with the solid line fit assuming contributions from both spin S = 2 and spin $S = 1$. The spin Hamiltonian parameters found from the fit were as follows: 25% $S = 2$, dashed line, $D = 9.5$ cm$^{-1}$, $E/D = 0.22$, $g = 2.3$; 75% $S = 1$, dot/dashed line, $D = 18.2$ cm$^{-1}$, $E/D = 0.09$, $g = 2.0$. The dominance of spin $S = 2$ over the spin $S = 1$ contribution to the magnetization despite the fact there are 3 times as many spin $S = 1$ sites as spin $S = 2$ sites is due to the larger $g$ value and smaller $D$ value for the spin 2 contribution.

having a spin $S = 2$. The goodness of fit parameter ($\chi_R^2$) (Day, 1993) indicates an excellent fit for the spin $S = 2$ only fit to the slow enzyme ($\chi_R^2 = 1.5$). The spin $S = 2$ only fit to the fast enzyme is of much lower quality ($\chi_R^2 > 8$) and improves dramatically ($\chi_R^2 < 2$) when both spin $S = 2$ and spin $S = 1$ are assumed to be present. Parameters derived from fitting both samples of both fast and slow oxidized cytochrome *c* oxidase are summarized in Table I.

Table I: Magnetic Properties of the $a_3$:$Cu_B$ Sites of Fast and Slow Cytochrome *c* Oxidase: Strong Exchange Coupling Limit

| | fast | | | | slow | | |
|---|---|---|---|---|---|---|---|
| $S$ | $D^a$ (cm$^{-1}$) | $g$ | $S$/protein (%) | $S$ | $D^a$ (cm$^{-1}$) | $g$ | $S$/protein (%) |
| | | | Sample 1 | | | | |
| both 2 | 5 (2) | 2.2 (2) | 35 (5)[b] | | | | |
| and 1 | 18 (1) | 2.0 (1) | 65 (5)[b] | | | | |
| only 2[c] | 7 (3) | 2.2 (1) | 70 (10) | 2 | −6 (2) | 2.0 (1) | 100 |
| | | | Sample 2 | | | | |
| both 2 | 10 (4) | 2.2 (2) | 30 (5)[b] | | | | |
| and 1 | 18 (1) | 2.0 (1) | 70 (5)[b] | | | | |
| only 2[c] | 11 (4) | 2.0 (1) | 80 (10) | 2 | −6 (1) | 2.0 (1) | 100 |

[a] Values of $E/D$ are soft and are not stated in this table. The stated uncertainties in the other parameters (in parentheses) are consistent with $E/D$ varying over the full range from 0 to $1/3$. The quality of fit varied from $\chi^2 \approx 1.4$ to 4 within this range of $E/D$ values. [b] The fact that the amounts of the spin $S = 1$ and spin $S = 2$ components add to 100% of the protein is, in part, a consequence of the relatively large number of fitting parameters being used in this model of the fast enzyme. [c] The quality of fit to the $a_3$:$Cu_B$ site of the fast enzyme assuming a single-spin $S = 2$ was substantially less ($\chi^2 \approx 8$) than for the same single-spin $S = 2$ fit to the $a_3$:$Cu_B$ site of the slow enzyme ($\chi^2 \approx 1.5$). This was the primary reason for modeling the $a_3$:$Cu_B$ site of the fast enzyme with two spins.

The speculative spin $S = 1$ component of the fast preparation could arise in either one of two ways. Either there is strong antiferromagnetic coupling between an intermediate-spin $S = 3/2$ ferric cytochrome $a_3$ site and the spin $S = 1/2$ cupric $Cu_B$ site, or there is strong ferromagnetic coupling between a low-spin $S = 1/2$ ferric cytochrome $a_3$ and the spin $S = 1/2$ cupric $Cu_B$ site. Of these two alternatives, the former is more plausible because ferromagnetic coupling within binuclear centers is rarely if ever strong (Kahn, 1987). There is evidence both for intermediate-spin ferric cytochrome $a_3$ in cytochrome *c* oxidase (Carter et al., 1981) and for low-spin ferric cytochrome $a_3$(Rusnak et al., 1987) in oxidized cytochrome *c* oxidase. Moreover, the distribution of the two spin states (75%:25% $S = 1$:$S = 2$ ratio) parallels the previously observed heterogeneity in reactivity with NO of fast samples (70%:20%:10%) (Palmer et al., 1988).

If verified, the suggestion that cytochrome $a_3$ is a mixture of both high-spin and intermediate-spin states would provide an explanation of the well-established result that the fast-to-slow conversion is accompanied by a blue-shift in the position of the Soret maximum, by as much as 7 nm (Baker et al., 1987). This shift is often said to be due to a low-spin to high-spin conversion of cytochrome $a_3$ (Moody et al., 1991). However, every parameter examined which should respond to a change in the low-spin component fails to detect any such process; these include Soret and near-infrared magnetic circular dichroism measurements (Baker et al., 1987) and resonance Raman spectra (Schoonover et al., 1988). The presence of an intermediate-spin to high-spin conversion would be consistent with all of the data.

*Weak Antiferromagnetic Exchange Coupling.* The data shown in Figure 2 can be fit as well with a very different model in which the exchange coupling between the high-spin $S = 5/2$ ferric cytochrome $a_3$ and the spin $S = 1/2$ cupric $Cu_B$ is very weak. Table II summarizes the parameters derived from fits to both preparations of both fast and slow samples using this weak exchange coupling model. The basic difficulty with this model is that the amount of $a_3$:$Cu_B$ site derived from the fit (last column of Table II) is substantially less than the amount of protein in the sample. For this competing model to hold, a substantial fraction of the cytochrome $a_3$ ferric iron would have to be present as low-spin $S = 1/2$ and very strongly

Table II: Magnetic Properties of the $a_3$:$Cu_B$ Sites of Fast and Slow Cytochrome *c* Oxidase: Weak Exchange Coupling Limit

| sample | $g(1/2)$ | $D(5/2)$ ($cm^{-1}$) | $E/D(5/2)$ | $g(5/2)$ | $J^a$ ($cm^{-1}$) | amount (nmol) of protein | amount (nmol) of background[b] | amount (nmol) of dimer | dimer/protein amount (%) |
|---|---|---|---|---|---|---|---|---|---|
| 1, fast | 2.04 | 3 | 0.1 | 2.0 | 3.4 | 62 | 43 | 23 | 37 |
| 2, fast | 2.04 | 10 | 0.1 | 2.0 | 3.0 | 48 | 45 | 26 | 55 |
| 1, slow | 2.01 | 1 | 0.0 | 2.06 | 4.2 | 55 | 39 | 34 | 62 |
| 2, slow | 2.00 | 1 | 0.0 | 2.10 | 3.6 | 53 | 53 | 35 | 66 |

[a] The exchange coupling term in the Hamiltonian is $J\mathbf{S_1}\cdot\mathbf{S_2}$. [b] $S = {}^1/_2$ signals from cytochrome *a* and $Cu_A$.

coupled to the spin $S = {}^1/_2$ cupric $Cu_B$ site yielding a diamagnetic center. In the absence of direct evidence for this low-spin ferric cytochrome $a_3$, we favor the strong coupling model.

The magnetic properties of the reduced form of the fast enzyme were observed to be spin $S = 2$ with $D = 14$ (5) $cm^{-1}$, $E/D = 0.20$ (5), and $g = 2.2$ (1). The uncertainties were found by averaging the results obtained by fitting data collected from two independent preparations of the fast enzyme. These measurements are consistent with previous studies of the reduced enzyme (Tweedle et al., 1978).

The results of this study are surprising. High spin-ferric hemes generally have large and positive $D$ values ($5 < D < 15$ $cm^{-1}$) with small $E/D$ (<0.1) values. Positive $D$ values indicate the in-plane interactions between the porphyrin macrocycle and the iron are stronger than the axial interactions (Mitra, 1983). $E/D$ values are generally small because high-spin Fe(III) sites in hemes are almost purely axial (Palmer, 1983). The negative $D$ value of the best fits to the slow enzyme therefore indicates a rare case where the axial interactions are stronger than the in-plane interactions, presumably as a result of a shortening of the bond between the heme iron and the putative bridging ligand. The relatively large $E/D$ values for the best fits to the spin $S = 2$ component of the fast enzyme and to the spin $S = 2$ slow enzyme indicate unusually large distortions from axial symmetry for the high-spin Fe(III) site of heme $a_3$. The large $D$ values are consistent with a high-spin Fe(III) site and are inconsistent with the Fe(IV) site in the model favored by Hagen (1982) and by Cooper and Salerno (Cooper et al., 1992) which would be expected to have a small $D$ value.

## CONCLUSIONS

Saturation magnetization data for the $a_3$:$Cu_B$ site of fast and of slow oxidized cytochrome *c* oxidase clearly distinguish these preparations as different in their magnetic properties.

Both the strong coupling and the weak coupling model can fit the form of the saturation magnetization data. The strong coupling model is favored since it results in a match between the amount of spin $S = 2$ paramagnetism found from the fit and the amount of protein determined spectroscopically to be in the sample.

The saturation magnetization data of the $a_3$:$Cu_B$ sites of both fast and slow oxidized cytochrome *c* oxidase can be approximated by spin $S = 2$ paramagnetism arising from high-spin $S = {}^5/_2$ Fe(III) tightly coupled antiferromagnetically (>100 $cm^{-1}$ $\mathbf{S_1}\cdot\mathbf{S_2}$) to $S = {}^1/_2$ Cu(II).

An improved fit to the saturation magnetization data of the $a_3$:$Cu_B$ site of fast but not of slow oxidized cytochrome *c* oxidase is obtained assuming a majority of the sample is spin $S = 1$ (75%, $S = 1$) with a fraction of the sample spin $S = 2$ (25%, $S = 2$).

The large values of $E/D$ for the best fits to both forms of the enzyme indicate unusually large distortions from axial symmetry for the heme $a_3$ site. The change in the sign of $D$ which accompanies the fast-to-slow transition in the best fits to the data implies a change in the axial ligation of the $a_3$ site.

## ACKNOWLEDGMENT

We thank Dr. Linda L. Pearce for help in analyzing the data.

## REFERENCES

Baker, G. M., Noguchi, M., & Palmer, G. (1987) *J. Biol. Chem. 262*, 595–604.

Barnes, Z. K., Babcock, G. T., & Dye, J. L. (1991) *Biochemistry 30*, 7597–7603.

Brudvig, G. W., Stevens, T. H., Morse, R. H., & Chan, S. I. (1981) *Biochemistry 20*, 3912–3921.

Brudvig, G. W., Morse, R. H., & Chan, S. I. (1986) *J. Magn. Reson. 67*, 189–201.

Carter, K. R., Antalis, T. M., Palmer, G., Ferris, N. S., & Woodruff, W. H. (1981) *Proc. Natl. Acad. Sci. U.S.A. 78*, 1652–1655.

Cooper, C. E., & Salerno, J. C. (1992) *J. Biol. Chem. 267*, 280–285.

Day, E. P. (1993) *Methods Enzymol. 227*, 437–463.

Day, E. P., Kent, T. A., Lindahl, P. A., Münck, E., Orme-Johnson, W. H., Roder, H., & Roy, A. (1987) *Biophys. J. 52*, 837–853.

Hagen, W. R. (1982) *Biochim. Biophys. Acta 708*, 82–98.

Hagen, W. R., Dunham, W. R., Sands, R. H., Shaw, R. W., & Beinert, H. (1984) *Biochim. Biophys. Acta 765*, 399–402.

Hendrich, M. P., & Debrunner, P. G. (1989) *Biophys. J. 56*, 489–506.

Hendrich, M. P., Pearce, L. L., Que, L., Jr., Chasteen, N. D., & Day, E. P. (1991) *J. Am. Chem. Soc. 113*, 3039–3044.

Kahn, O. (1987) *Struct. Bonding 68*, 89–167.

Kent, T. A., Münck, E., Dunham, W. R., Filter, W. F., Findling, K. L., Yoshida, T., & Fee, J. A. (1982) *J. Biol. Chem. 257*, 12489–12492.

Mitra, S. (1983) *Iron Porphyrins, Part II* (Lever, A. B. P., & Gray, H. B., Eds.) pp 1–42, Addison-Wesley Publishing Co., Reading, MA.

Moody, A. J., Cooper, C. E., & Rich, P. R. (1991) *Biochim. Biophys. Acta 1059*, 189–207.

Moss, T. H., Shapiro, E., King, T. E., Beinert, H., & Hartzell, C. (1978) *J. Biol. Chem. 253*, 8072–8073.

Naqui, A., Kumar, C., Ching, Y.-C., Powers, L., & Chance, B. (1984) *Biochemistry 23*, 6222–6227.

Palmer, G. (1983) *Iron Porphyrins, Part II* (Lever, A. B. P., & Gray, H. B., Eds.) pp 43–88, Addison-Wesley, Reading, MA.

Palmer, G., Baker, G. M., & Noguchi, M. (1988) *Chem. Scr. 28A*, 41–46.

Rusnak, F. M., Münck, E., Nitsche, C. I., Zimmermann, B. H., & Fee, J. A. (1987) *J. Biol. Chem. 262*, 16328–16332.

Scaringe, R. P., Hodgson, D. J., & Hatfield, W. E. (1978) *Mol. Phys. 35*, 701–713.

Schoonover, J. R., Dyer, R. B., Woodruff, W. H., Baker, G. M., Noguchi, M., & Palmer, G. (1988) *Biochemistry 27*, 5433–5440.

Tweedle, M. F., Wilson, L. J., Garcia-Iñiguez, L., Babcock, G. T., & Palmer, G. (1978) *J. Biol. Chem. 253*, 8065–8071.

Van Buuren, K. J. H., Nicholls, P., & Van Gelder, B. F. (1972) *Biochim. Biophys. Acta 256*, 258–276.

Wang, H., Sauke, T., Debrunner, P. G., & Chan, S. I. (1988) *J. Biol. Chem. 263*, 15260–15263.